THE ASTROPHYSICAL JOURNAL, 896:153 (12pp), 2020 June 20 https://doi.org/10.3847/1538-4357/ab9083
© 2020. The American Astronomical Society. All rights reserved.

ACRONYM IV: Three New, Young, Low-mass Spectroscopic Binaries

Laura Flagg[1,2,3], Evgenya L. Shkolnik[4], Alycia Weinberger[5], Brendan P. Bowler[6], Brian Skiff[3], Adam L. Kraus[6], and Michael C. Liu[7]

[1] Department of Physics and Astronomy, Rice University, 6100 Main St. MS-108, Houston, TX 77005, USA; laura.flagg@rice.edu
[2] Department of Physics and Astronomy, Northern Arizona University, Box 6010, Flagstaff, AZ 86011, USA
[3] Lowell Observatory, 1400 W Mars Hill Road, Flagstaff, AZ 86001, USA
[4] School of Earth and Space Exploration, Arizona State University, 781 S Terrace Road, Tempe, AZ 85281, USA
[5] Department of Terrestrial Magnetism, Carnegie Institution for Science, 5241 Broad Branch Road, NW, Washington, DC 20015, USA
[6] McDonald Observatory and the Department of Astronomy, The University of Texas at Austin, Austin, TX 78712, USA
[7] Institute for Astronomy, University of Hawai'i Mânoa, 2680 Woodlawn Drive, Honolulu, HI 96822, USA
Received 2019 October 10; revised 2020 May 4; accepted 2020 May 4; published 2020 June 23

Abstract

As part of our search for new low-mass members of nearby young moving groups (YMGs), we discovered three low-mass, spectroscopic binaries, two of which are not kinematically associated with any known YMG. Using high-resolution optical spectroscopy, we measure the component and systemic radial velocities of the systems, as well as their lithium absorption and Hα emission, both spectroscopic indicators of youth. One system (2MASS J02543316−5108313, M2.0+M3.0) we confirm as a member of the 40 Myr old Tuc-Hor moving group, but whose binarity was previously undetected. The second young binary (2MASS J08355977−3042306, K5.5+M1.5) is not a kinematic match to any known YMG, but each component exhibits lithium absorption and strong and wide Hα emission indicative of active accretion, setting an upper age limit of 15 Myr. The third system (2MASS J10260210 −4105537, M1.0+M3.0) has been hypothesized in the literature to be a member of the 10 Myr old TW Hya Association, but our measured systemic velocity shows the binary is in fact not part of any known YMG. This last system also has lithium absorption in each component, and has strong and variable Hα emission, setting an upper age limit of 15 Myr based on the lithium detection.

Unified Astronomy Thesaurus concepts: Low mass stars (2050); Spectroscopic binary stars (1557); Stellar associations (1582); Stellar evolution (1599); Pre-main sequence stars (1290); Stellar classification (1589); M dwarf stars (982); K dwarf stars (876); Stellar kinematics (1608); High resolution spectroscopy (2096); Radial velocity (1332)

1. Introduction

Finding and characterizing young, low-mass stars has become a prominent research focus in recent years. There is interest in finding sub-stellar companions, especially planets, around young low-mass stars to provide observational constraints for planet formation (Crockett et al. 2012; Spiegel & Burrows 2012). As low-mass stars are the most common planet host (e.g., Dressing & Charbonneau 2013), finding these stars provides targets for potential planet searches. Additionally, characterizing young, low-mass stars is important to accurately infer the properties of any planets around them. And as low-mass stars (late K and M stars) with masses less than $\sim$0.7 $M_{\odot}$ comprise more than 75% of the stellar population (Reid & Gizis 1997; Bochanski et al. 2010), understanding the early evolutionary stages of low-mass stars is critical for understanding the stellar population as a whole (Dib 2014).

The first step to widening our understanding is identifying these smaller—and fainter—young stars. Young moving groups (YMGs) are kinematically linked stars that formed together but have since dispersed (e.g., Zuckerman & Song 2004). The properties of the group as a whole can be used to age-date the stars. Over the past three decades, YMGs have been discovered based on kinematics with ages between $\sim$8 and 300 Myr old (Torres et al. 2006). In recent years, more low-mass members have been added to these groups by looking for kinematics and age indicators matched to known higher-mass members (e.g., Montes et al. 2001; Schlieder et al. 2010, 2012; Shkolnik et al. 2011, 2012; Malo et al. 2014; Gagné et al. 2015; Liu et al. 2016; Bowler et al. 2019). Since we expect 3 of every 4 of the members to be M dwarfs, as in the rest of the galaxy, there are many more low-mass stars to be found. Until they are, the census of the stellar population is incomplete.

In order to address the issue of incomplete stellar population for YMGs, the All-sky Co-moving Recovery Of Nearby Young Members (ACRONYM) search was created. Thus far, the program has classified 129 new low-mass members of the 40 Myr Tuc-Hor Moving Group (Kraus et al. 2014), 41 new low-mass members of the 23 Myr Beta Pic Moving Group (Shkolnik et al. 2017), and 77 members of other groups (Schneider et al. 2019).

2. Candidate Selection

The initial candidate selection process was the same as that of Shkolnik et al. (2017), which is based on identifying cool stars using 2MASS colors and magnitudes (Skrutskie et al. 2006), along with proper motions. As youth is well-correlated with chromospheric activity, and high chromospheric activity can be measured photometrically in the X-ray and ultraviolet (UV), surveys in the X-ray with ROSAT (Voges et al. 1999) and the UV with Galaxy Evolution Explorer (GALEX) (Martin et al. 2005) were cross-referenced with our list of cool stars.

The coordinates and proper motions of stars from this list were also used as criteria. Certain combinations make it more likely for a star to be a kinematic fit into a YMG. For each star, the full kinematics were calculated with different possible

Table 1
Targets and Their Parameters from Literature

Object	R.A.	Decl.	Spectral Type	$\mu_{\mathrm{R.A.}}$ (mas yr^{-1})	$\mu_{\mathrm{Decl.}}$ (mas yr^{-1})	V Mag	Distance (pc)	FUV (μJy)	NUV (μJy)	HR1	HR2
J02543316−5108313	02 54 33.16	−51 08 31.4	M1.1	93.5	−11.8	12.1	44.3	21.5	79.4	⋯	⋯
J08355977−3042306	08 35 59.77	−30 42 30.7	K4	−64.2	−14.5	11.3	62.9	⋯	⋯	0.15	−0.20
J10260210−4105537	10 26 02.11	−41 05 53.7	M0.5	−46.4	−1.8	12.6	84.9	16.5	113.6	⋯	⋯

Note. V magnitudes are from Zacharias et al. (2013). Composite spectral types are from Kraus et al. (2014) for J02543316−5108313, Torres et al. (2006) for J08355977−3042306, and Riaz et al. (2006) for J10260210−4105537. Distances and proper motions are from Gaia (Brown et al. 2018). UV flux densities are from GALEX (Bianchi et al. 2011). J08355977−3042306 was not observed with GALEX. Hardness ratios (HR) are from ROSAT (Voges et al. 1999).

radial velocities and distances for that star, along with the known coordinates and proper motions for that star. Stars where no plausible combination of distance and radial velocity allowed for membership were removed from our list, as in Kraus et al. (2014).

After selecting for UV or X-ray activity, we follow up with high-resolution spectroscopic observations to measure radial velocities and spectroscopic youth indicators. Further follow up observations were carried out to search for radial velocity (RV) variability. In our activity-selected sample, we found three spectroscopic binaries (SBs) that also display signatures of youth (Table 1). Binary stars are especially important to identify because they provide some of the best opportunities to calibrate stellar models and their predictions of fundamental stellar characteristics. Measuring fundamental properties is crucial for understanding young, low-mass stars, as they are not currently well modeled (Feiden & Chaboyer 2012; Somers & Pinsonneault 2015).

3. Targets

Previous studies found evidence that all three of the spectroscopic binaries we analyze in this work are young. However, none of these objects had been identified as a binary system.

3.1. 2MASS J02543316−5108313

2MASS J02543316−5108313, also identified as GSC 08057 −00342, was observed by Torres et al. (2000) in a search for a new young moving group near the active young star ER Eri. Despite physical proximity and similar proper motions, 2MASS J02543316−5108313 was not classified into this new group called the Horologium association. Rodriguez et al. (2013) later determined there was a >99% chance that the star was in this association, now referred to as Tuc-Hor, based on its location and proper motion. Kraus et al. (2014) measured the radial velocity as 13.8 ± 0.4 km s^{-1} which confirmed that membership, but did not identify it as an SB2, as the lines were blended during the epoch of their observation.

This system was imaged by Bergfors et al. (2010) in a search for binaries, but no visual components were detected down to 0.″1. This was followed up by Janson et al. (2012), who classified it as a single star with X-ray emission. Krzesinski et al. (2012) measured a light curve of the system in a search for variability, but no periodicity was detected nor were any flares. Gaia DR2 (Brown et al. 2018) indicates that it has a proper motion companion with a 15″ separation, which has an RV consistent with that of Tuc-Hor. Shan et al. (2017) identified binaries with separations as low as 40 mas using MagAO, but did not detect another companion to this star that could potentially complicate the analysis of the system's kinematics. Its spectral type in the literature ranges from M1.1 (Kraus et al. 2014) to M3 (Torres et al. 2000). A low-resolution optical spectra from 2014 was presented in Bowler et al. (2019). They found a spectral type of M0 and an Hα equivalent width (EW) of -3.2 ± 0.3 Å.

3.2. 2MASS J08355977−3042306

2MASS J08355977−3042306, also referenced as CD-30 6530, was previously identified as a pre-main sequence K4Ve star by Torres et al. (2006), who also measured lithium absorption with an EW of 230 mÅ and an RV of 6.8 km s^{-1}. It was detected by ROSAT in the X-ray (Voges et al. 1999). We observed it as part of a search for possible 23 Myr βPMG members (Shkolnik et al. 2017).

3.3. 2MASS J10260210−4105537

We initially observed J10260210−4105537, an M0.5 star, due to two youth indicators indicators: X-ray emission and a strong Hα EW of −6.9 Å (Riaz et al. 2006). In a search for TW Hya Association (TWA) members, Rodriguez et al. (2011) observed the system based on GALEX UV data. Their high-resolution spectrum showed lithium absorption, with an EW of 500 ± 70 mÅ. They also measured a spectral type of M1. However, they did not identify the binarity of the system. A photometric survey by Janson et al. (2012) did not resolve the binary either and marked the system as a single star. Kiraga (2012) analyzed the light curve from ASAS, which is a photometric survey with a resolution of 15″ (Pojmanski 2002); they calculated a 0.42 day periodicity that they attributed to rotation and noted it was blended with a nearby star. Naud et al. (2017) looked for a potential companion at large separations and found none. Gagné et al. (2017) classify it as a likely contaminant to TWA, and that its true membership is in the Lower Centaurus Crux. Bowler et al. (2019) measure a spectral type M2 and a lithium EW of 410 mÅ based on low-resolution spectroscopy; while they indicate that TWA is its most likely association, they acknowledge the need for a RV measurement.

4. High-resolution Optical Spectra

4.1. Observations

In order to confirm group membership, we measured a radial velocity and youth indicators by using high-resolution optical spectroscopy. Fourteen spectra in total were taken of the candidates between 2009 June and 2017 July from three different telescopes. We aimed for a signal-to-noise ratio (S/N) of 25–30 at 7000 Å (Table 2).

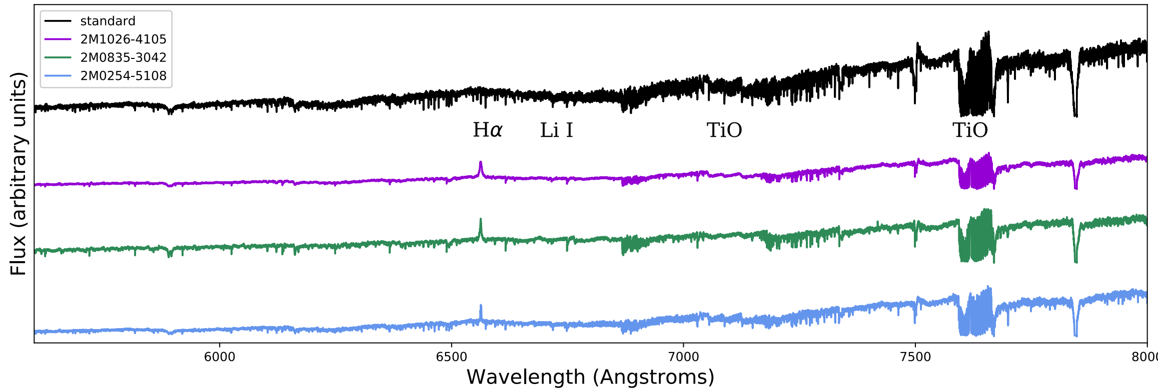

Figure 1. Samples of the relevant portion of the spectra for our targets taken with the echelle spectrograph on the du Pont telescope on 2015 December 11. The example standard star shown is GJ 908.

Table 2
Spectroscopic Observations

Object	UT Date	Telescope	Integration Time (s)	HJD
J02543316−5108313	2009 Aug 23	du Pont	600	2455066.91963418
J02543316−5108313	2015 Jun 22	du Pont	1350	2457196.91753853
J02543316−5108313	2015 Dec 11	du Pont	750	2457367.60084198
J08355977−3042306	2014 Mar 18	du Pont	400	2456744.59019459
J08355977−3042306	2015 Jan 12	du Pont	800	2457035.77692500
J08355977−3042306	2015 Feb 17	SMARTS	400	2457079.71270571
J08355977−3042306	2015 Dec 11	du Pont	1200	2457367.81581571
J08355977−3042306	2017 Jul 3	du Pont	1200	2457937.44805283
J10260210−4105537	2009 Jun 14	du Pont	900	2454996.54189175
J10260210−4105537	2009 Dec 31	Clay	150	2455196.70946915
J10260210−4105537	2010 Dec 29	Clay	100	2455559.69428480
J10260210−4105537	2011 Jun 14	Clay	40	2455727.46221318
J10260210−4105537	2015 Dec 11	du Pont	1200	2457367.85578601
J10260210−4105537	2015 Dec 13	du Pont	900	2457369.83365365

Most of our spectra were taken on the 2.5 m Irénée du Pont telescope at Las Campanas Observatories using the echelle spectrograph.[8] The detector is a SITe2k CCD with 24 μm pixels mounted at the Cassegrain focus. We used a $0\farcs75 \times 4''$ slit, which results in a spectral resolution of ≈40,000 over 57 orders from 3625 to 9325 Å (Figure 1). We acquired "milky" flat field images at twilight every night, created using a diffuser behind the slit, which distributes the light evenly across the detector. We took Th–Ar spectra immediately following each observation in order to minimize variations from the spectrum. The images were reduced using the standard IRAF tasks (Tody 1986).

We obtained one spectrum with the CHIRON spectrograph (Tokovinin et al. 2013), which is mounted on the Cerro Tololo Inter-American Observatory's 1.5 m Small and Moderate Aperture Research Telescope System (SMARTS) 1.5 m telescope (NOAO Proposal ID: 2015A-0016; PI: B. Bowler). This spectrum has 62 orders, with a spectral resolution of ≈28,000 and covers wavelengths between 4500 and 8900 Å. The spectrum was taken in queue mode. The reduction, comprising a bias subtraction, flat-fielding, order extraction, and wavelength calibration using Th–Ar, was done using the automated reduction pipeline.

For one target (2MASS J10260210−4105537), we obtained spectra taken on the Clay 6.5 m telescope at Las Campanas Observatories, using the Magellan Inamori Kyocera Echelle (MIKE) spectrograph (Bernstein et al. 2003). A $0\farcs5$ slit was used to achieve a spectral resolution of ≈35,000 between 4900 and 10000 Å. These spectra were reduced using the facility pipeline (Kelson 2003), which uses a milky flat to flat field the image, then extracts and calibrates the spectra. Th–Ar spectra were used for wavelength calibration. Additional adjustments to the wavelength calibration, typically less than 0.5 km s^{-1}, were made using the telluric molecular oxygen *A* band between 7620 and 7660 Å.

4.2. Spectral Types and Masses

For calculating spectral indices, the blaze function was removed and the orders were combined to create one-dimensional spectra. The IRAF task *sbands* was used to calculate the indices used for spectral typing the targets.

For the MIKE data, we used the TiO5 index, which, as defined by Reid et al. (1995), is the ratio of the average flux from 7126 to 7135 Å, covering the TiO band, to the average

[8] http://www.lco.cl/telescopes-information/irenee-du-pont/instruments/website/echelle-spectrograph-manuals/echelle-spectrograph-users-manual

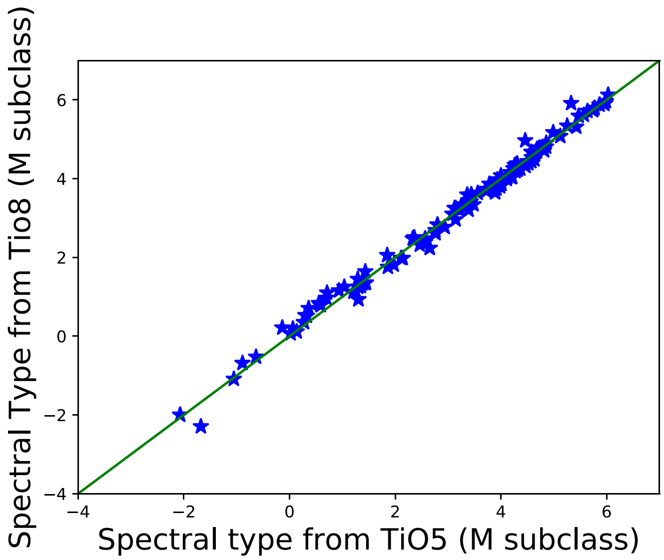

Figure 2. Comparison of the TiO5 index with the TiO8 index for 141 low-mass stars observed with MIKE.

continuum flux from 7042 to 7046 Å. This is then converted into a spectral type (SpT) by the empirically derived function:

$$\mathrm{SpT} = -10.775 \times \mathrm{TiO5} + 8.2 \tag{1}$$

where SpT is the M subclass (with −1 and −2 corresponding to K7 and K5, respectively) and TiO5 is the flux ratio. It has an uncertainty of 0.5 subclasses.

Since the spectra from the du Pont have the continuum of the index very close to the end of an order, we devised a variation of the TiO5 index for calculating spectral types of late K and early M stars for these spectra. Instead of using the 7042–7046 Å region for a continuum, the region from 7558 to 7562 Å—which is also a continuum (Kirkpatrick et al. 1991)—is used. The average flux from 7126 to 7135 Å is divided by the average flux from 7558 to 7562 Å and this ratio, henceforth known as TiO8, is converted into a spectral type by

$$\mathrm{SpT} = 5.3 \times \mathrm{TiO8}^2 - 15.2 \times \mathrm{TiO8} + 7.2. \tag{2}$$

The resulting spectral types fit very closely with TiO5 for a sample of 141 MIKE spectra of low-mass stars (Figure 2). The residual standard error for this fit is 0.167, and combining this with the TiO5 uncertainty, the overall uncertainty for TiO8 is 0.5 spectral subclasses. Due to intrinsic uncertainty, we round all spectral types to the nearest 0.5 subclass.

To calculate the spectral type of the individual components, we started with a grid of potential masses between 1.0 and 0.08 $M_\odot$ in increments of 0.01 $M_\odot$. We then converted masses to spectral types using relations derived by Pecaut & Mamajek (2013) and Baraffe et al. (2015), interpolating for values not explicitly calculated for. We normalized both the masses and the spectral types to account for the fact that they do not have the same units. We created a grid of component pairings that included masses and spectral types for each individual component. We calculated the composite spectral type weighted by *I*-band fluxes and mass ratio for each pairing. The final component spectral types and masses were the ones that minimized the differences between the measured composite spectral type and mass ratio simultaneously.

Table 3
The RV Standards Used for Cross-correlation

Star	Spectral Type	RV (km s^{-1})
GJ 156	K7	62.6
GJ 273	M3.5	18.3
GJ 388	M4.5	12.4
GJ 406	M4	19.5
GJ 433	M1.5	18.0
GJ 514	M0.5	14.6
GJ 653	K5	34.1
GJ 699	M4	−110.5
GJ 908	M1	−71.1

Note. Radial velocities for the standards are from Nidever et al. (2002) and have uncertainties of 0.15 km s^{-1}.

4.3. Radial Velocities

As the initial purpose for acquiring the spectra was to find new young moving group members by kinematics, we measure radial velocities for our stars, using the cross-correlation function (CCF) (Tonry & Davis 1979). The new SBs were identified by their double-peaked CCFs.

To measure radial velocities of the individual components, we cross-correlated orders of the spectra with those of standard stars (Table 3) using the IRAF task *fxcor* (Fitzpatrick 1993). We found the peak by fitting a Gaussian to the CCF and finding the center of that Gaussian. We calculated uncertainties by combining the standard deviation of the velocities measured in each order with the uncertainty from wavelength calibration, calculated by the standard deviation from cross-correlating standards with other standards, and the uncertainty in the standards' RV of 0.15 km s^{-1}. The "A" component was taken to be the component with the higher CCF peak. For spectra where the stars were especially blended, our own program created in LabVIEW was used to fit the sum of two Gaussians to the CCF. This allowed us to have more control over the free parameters of the fit.

To calculate the systemic RV of these systems, we plotted the RV of the secondary component as a function of the RV of the primary component, as described in Wilson (1941). We then fit a straight line to the data using the *scipy.odr* module (Virtanen et al. 2019), which accounts for uncertainties in both dimensions. This can then be used to calculate the systemic RV and mass ratio, q.

4.4. UVW and XYZ

We calculated the three-dimensional UVW space velocities, following Johnson & Soderblom (1987), and the XYZ coordinates, following Murray (1989), with errors propagated from the uncertainties in the RV measurements and distances. The XYZ calculation requires a R.A., decl., and distance; the UVW calculation requires those values in addition to proper motions and radial velocities. Distances are calculated from Gaia DR2 parallaxes (Brown et al. 2018; Luri et al. 2018).

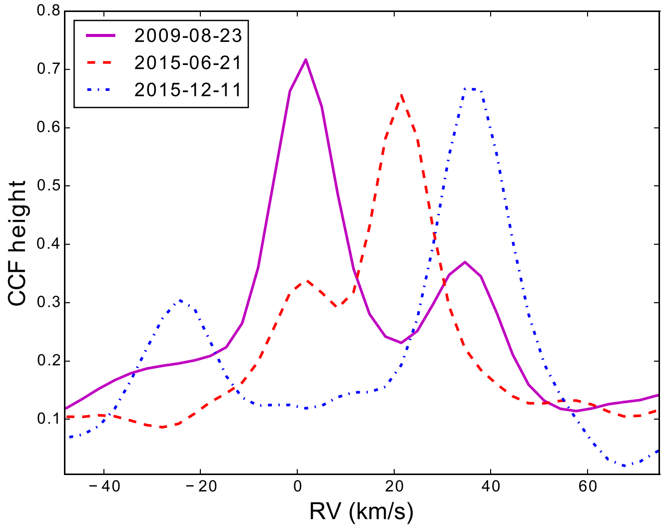

Figure 3. CCFs for 2MASS J02543316−5108313 show binarity, with two peaks in each epoch.

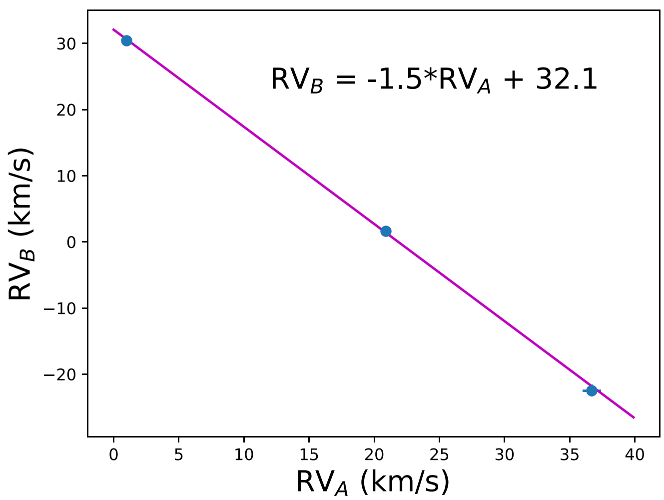

Figure 4. RV of component *B* plotted vs. the RV of component *A* for the SB2 2MASS J02543316−5108313 from spectra collected over three epochs.

4.5. Youth Indicators

There are various indicators with spectral and photometric data that can indicate a young age. The three that we considered with these objects are lithium absorption, IR excess, and Hα emission. The presence of lithium absorption in a stellar spectrum is an indication of youth, because lithium is depleted via convective mixing early in a star's life (Bonsack 1959; Bonsack & Greenstein 1960; Skumanich 1972). The precise age at which this happens depends on spectral type, but for low-mass stars, which have large convective zones, this age is typically between 15 and 45 Myr (Chabrier & Baraffe 1997).

Protoplanetary disks have lifetimes typically less than 10 Myr (Williams & Cieza 2011 and references therein). Therefore, any star with such a protoplanetary disk must be young, identified by near-infrared or mid-infrared excess. Additionally, a stellar spectrum can reveal accretion signatures, such as strong and broadened Hα emission (Barrado y Navascués & Martín 2003). Hα emission can also be the result of chromospheric activity, as younger stars are typically more active due to faster rotation periods (e.g., Skumanich 1972; Linsky 1980; Walter et al. 1988; Montes et al. 1997; Soderblom et al. 1998).

Table 4
RVs for the Two Components of 2MASS J02543316−5108313

UT Date	RV of *A* (km s^{-1})	RV of *B* (km s^{-1})
2009 Aug 23	1.0 ± 0.2	30.4 ± 0.7
2015 Jun 22	20.9 ± 0.2	1.6 ± 0.5
2015 Dec 11	36.7 ± 0.7	−22.5 ± 0.9

4.6. Binary Periods and Separations

While a complete orbit is needed to measure orbital elements and physical properties, we can determine the upper limits of both the separation and the period of the binary system using our data. The epoch in which the two components have the largest RV separation, ΔRV_{max}, can be used with Kepler's third law and the total mass of the system to calculate the upper limit for the period, P_{orb}, and semimajor axis, a.

5. Optical Photometric Monitoring

In addition to the high-resolution spectra, we obtained photometric observations to measure a rotation period. We acquired *V*-band photometric data of 2MASS J08355977−3042306 from 2015 and 2017 taken with Lowell Observatory's 0.7 m telescope in robotic mode. Two to three exposures of 70 s each were taken at each visit to the field with uncertainties generally around 0.003 mag. The field was typically visited two times per night. We have a total of 433 photometric observations.

Using the photometric data of 2MASS J08355977−3042306, we attempted to determine a rotation period of the stars using a Lomb–Scargle periodogram (Horne & Baliunas 1986). We analyzed all the data together and also separated by the year they were taken.

6. Results and Analysis

6.1. 2MASS J02543316−5108313

We acquired three spectra of 2MASS J02543316−5108313 from the du Pont telescope, each of which show two peaks in the CCF (Figure 3). We measured the RV of each peak in all three epochs (Table 4).

Based on our plot of the secondary's RV versus the primary's RV for this system (Figure 4), we calculated a systemic RV of 13.0 ± 0.1 km s^{-1} and a mass ratio of 0.68 ± 0.03. Based on the Gaia DR2 parallax (Brown et al. 2018), the system is at a distance of 43.8 pc. With this distance, we then calculated UVW velocities (see Table 5) consistent with the Tuc-Hor members (Malo et al. 2014), as shown in Figure 5, which have an expected age of 40 Myr.

Our measured composite spectral type for this system is an M2.2, which falls in the range of spectral types previously measured. Using this, the mass ratio, and an estimated age of 40 Myr, we simultaneously fit for the accurate mass ratio and the composite spectral type to get the individual component masses and spectral types. The primary component has a spectral type of M1.9, which we round to M2.0, and a mass of 0.40 $M_{\odot}$, while the secondary has a spectral type of M2.9,

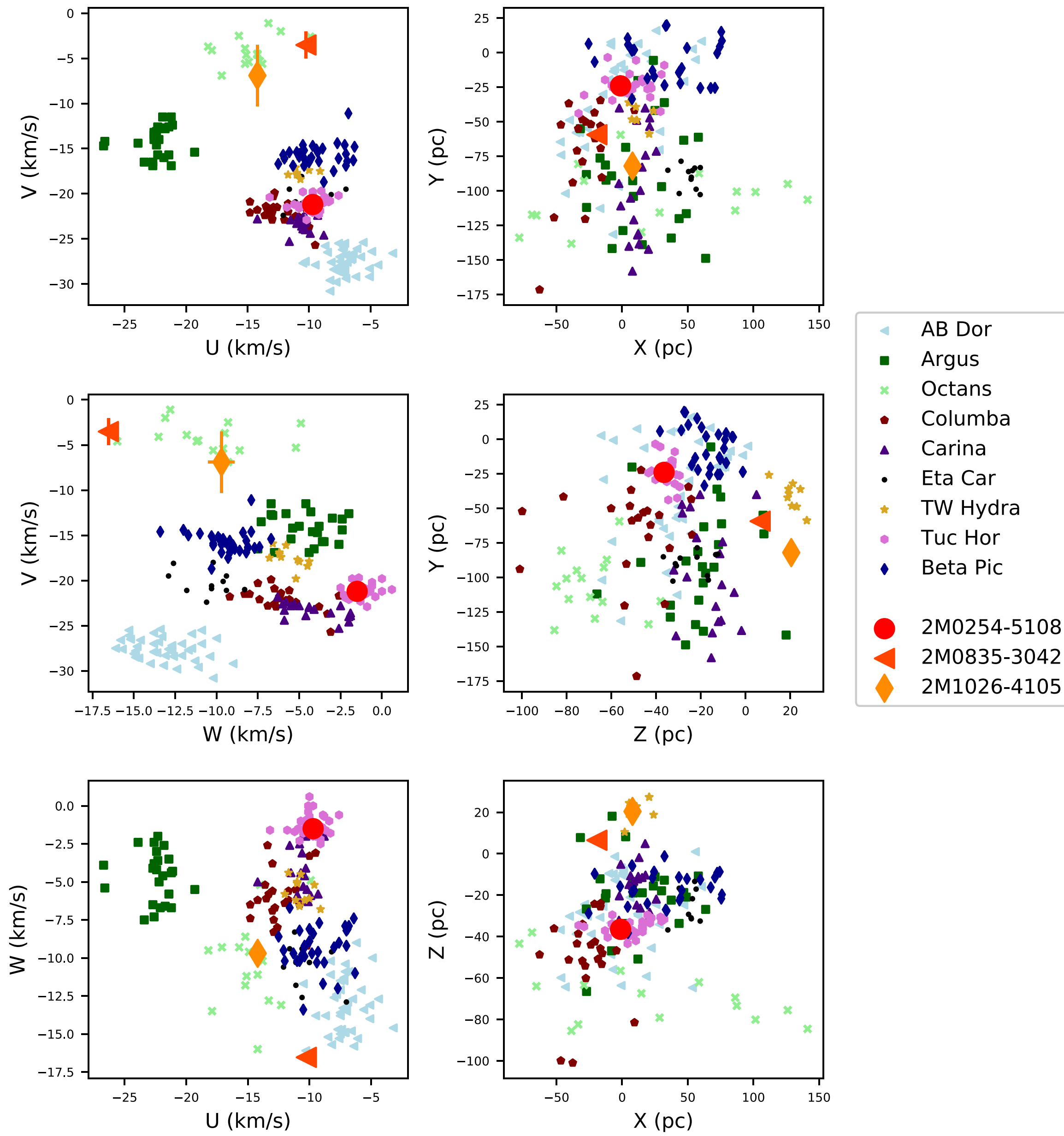

Figure 5. UVW velocities and XYZ coordinates of our target and YMG members put 2MASS J02543316−5108313 in the Tuc-Hor moving group. 2MASS J08355977−3042306 and 2MASS J10260210−4105537 do not appear to be a member of any of these groups.

Table 5
Kinematics and Orbital Parameters

Object	U (km s^{-1})	V (km s^{-1})	W (km s^{-1})	X (pc)	Y (pc)	Z (pc)	P_{orb} (days)	a (au)	q
2M0254−5108	−10.0 ± 0.1	−21.6 ± 0.1	−1.2 ± 0.1	−1.2 ± 0.1	−24.7 ± 1.7	−37.6 ± 2.8	<32.1	<0.17	0.68 ± 0.03
2M0835−3042	−9.9 ± 0.5	−3.6 ± 1.5	−15.8 ± 0.2	−18.4 ± 1.0	−56.4 ± 3.1	6.2 ± 0.3	<134.0	<0.56	0.59 ± 0.06
2M1026−4105	−14.2 ± 0.4	−6.79 ± 3.4	−9.7 ± 0.9	7.9 ± 0.1	−82.0 ± 1.0	20.4 ± 0.2	<9.4	<0.08	0.59 ± 0.30

which we round to M3.0, and a mass of 0.27 $M_{\odot}$. The lack of lithium from either component puts an additional lower age limit of 20 Myr on the system (Baraffe et al. 2015). The upper limits of the period and the semimajor axis are 32.1 days and 0.17 au, respectively.

6.2. 2MASS J08355977−3042306

We used the TiO8 index and measured a composite spectral type of K7.1 for 2MASS J08355977−3042306. This is a later spectral type than the previously measured one of K4 (Torres et al. 2006). However, the star has TiO absorption bands (Figure 6),

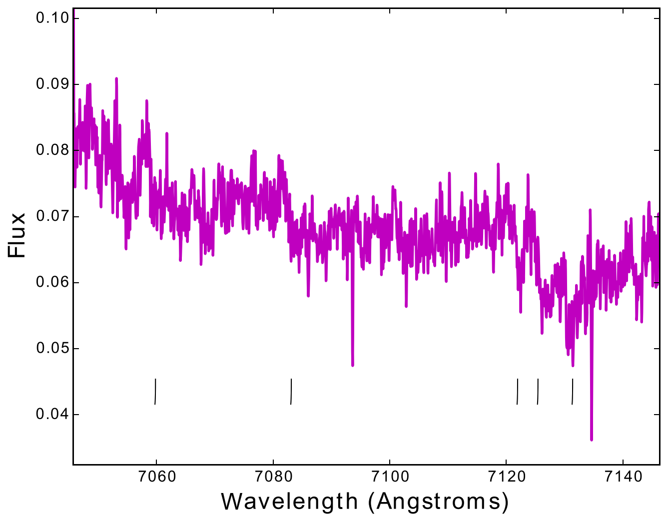

Figure 6. TiO absorption bands in the spectrum of 2MASS J08355977−3042306 (taken with the echelle spectrograph on the du Pont telescope on 2014 March 18) indicate that the composite spectral type is K5 or later.

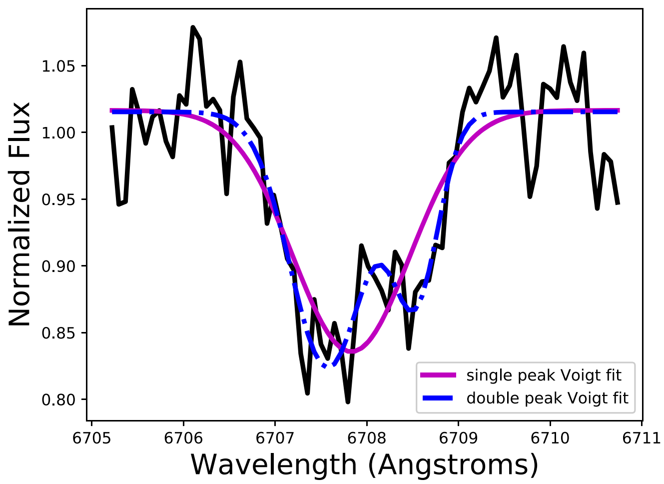

Figure 7. Models of the lithium absorption at 6708 Å for 2MASS J08355977−3042306 from the 2014 March 18 spectrum comparing the fit of a single peak vs. a double peak. The double peak fits better, even considering the additional free parameters.

which appear only in stars with spectral types of K5 or later (Reid et al. 1995), thus ruling out K4 as a possibility.

The lithium absorption line at 6708 Å (Figure 7) has a combined EW of 0.25 ± 0.10 Å, with the presence of lithium in both objects spectroscopically resolved.

We measured the EW of the Hα line at 6562.8 Å to be -3.0 ± 0.3 Å, in agreement with the value of -2.9 Å measured by Torres et al. (2006), using the standard convention that emission features have negative EWs. We also measured the 10% velocity width, defined as the full width of the line at 10% of the height (see Figure 8), to be $\sim$350 km s^{-1}. This width is indicative of accretion (White & Basri 2003). However, it should be noted that there is no obvious IR excess based on its 2MASS and WISE colors (Wright et al. 2010), which implies the system lacks warm dust (e.g., Spangler et al. 2001). It is possible that the system is accreting gas, which would not appear as IR excess (Hoadley et al. 2015).

To confirm 2MASS J08355977−3042306 is a binary and not a single star, we fit the lithium line with both a single peak and a double peak function using both Gaussian and Voigt models (see Figure 7). For both models, Bayesian Information Criteria (Kass & Raftery 1995)—which takes into account the number of free parameters—indicated that the double peak model clearly fit better, with a difference of 14.9 for the Gaussian and 10.6 for the Voigt.

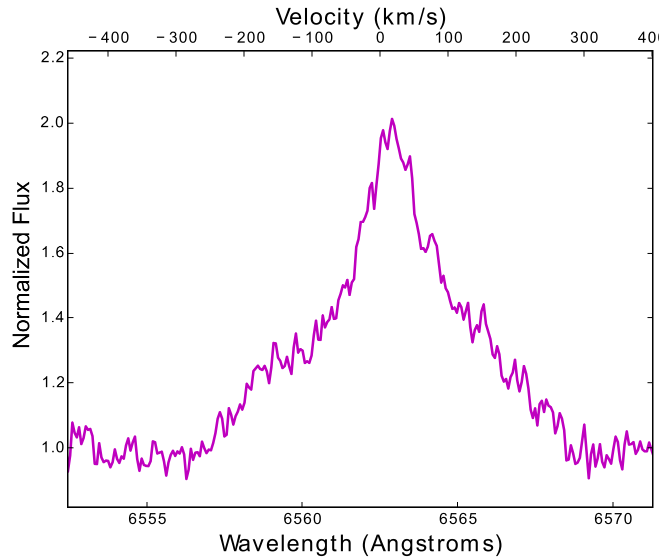

Figure 8. Hα emission for 2MASS J08355977−3042306 from 2014 March 18. The 10% velocity width is $\sim$350 km s^{-1}, which is typically indicative of accretion.

Table 6
RVs for 2MASS J08355977−3042306

UT Date	RV of A (km s^{-1})	RV of B (km s^{-1})
2014 Mar 28	-10.7 ± 3.9	34.7 ± 4.9
2015 Dec 11	12.9 ± 3.3	-27.4 ± 5.1

For two of the epochs, the CCF could be deblended into separate peaks (Figure 9). We measured the RVs of those peaks (Table 6), and then plotted our measurements (Figure 10). The resulting systemic RV is 4.7 ± 1.6 km s^{-1}; the mass ratio is 0.59 ± 0.06. Based on this mass ratio, the primary has a mass of 0.79 $M_\odot$, which corresponds to a spectral type of K5.4, which we round to K5.5, and the secondary has a mass of 0.46 $M_\odot$, which corresponds to a spectral type of M1.4, which rounds to M1.5. As lithium is depleted within 15 Myr for 0.4–0.5 $M_\odot$, stars (Baraffe et al. 2015), the system must be younger than that. The upper limit of the period is 134.0 days; the upper limit of the semimajor axis is 0.56 au.

The periodograms we calculated (Figure 11) all show periodicity at 0.32 day, around 1 day, and at 7.15 days. The peaks at 1 day are likely to be caused by the nature of sampling the data every night. The peaks at 0.32 day could be the rotation period of the primary. However, this would put its velocity close to the breakup speed. The peaks at 7.15 days may be a more physically realistic estimate of the rotation period, and thus the orbital period. Both the 0.32 day and the 7.15 day periods are within the range of rotation periods common for stars of this age (Rebull et al. 2018). Simulations suggest that tidal locking takes at minimum 15 Myr (Fleming et al. 2019), so we would not expect this to be reflective of the orbital period.

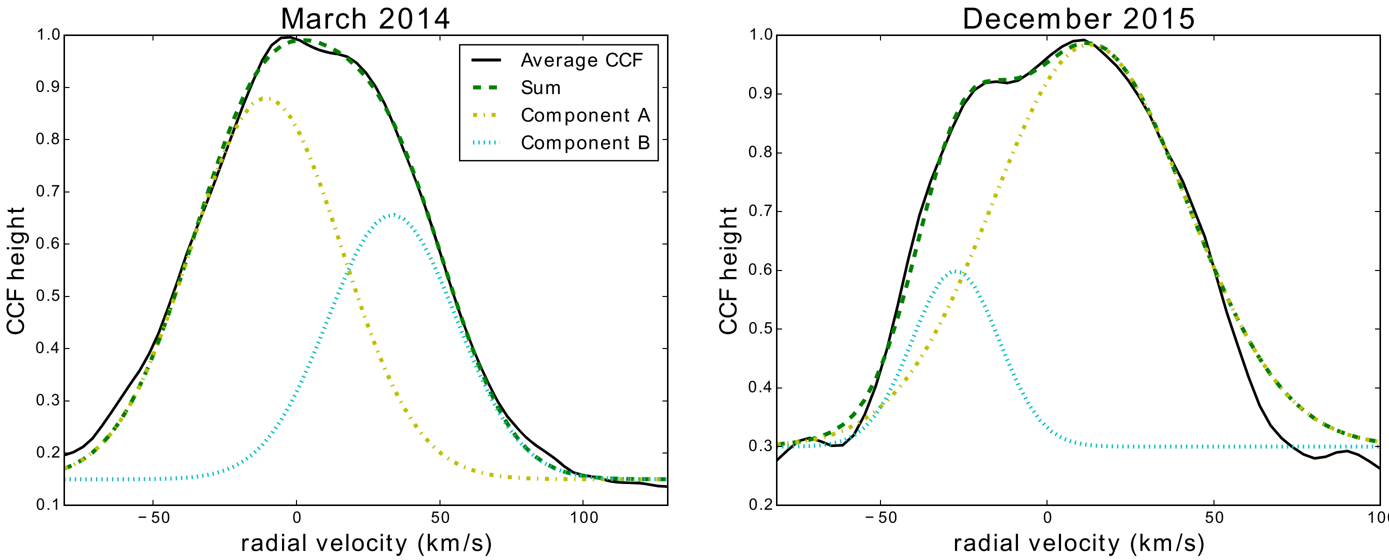

Figure 9. Deblended CCFs for 2MASS J08355977−3042306 on 2014 March 28 (left) and 2015 December 11 (right).

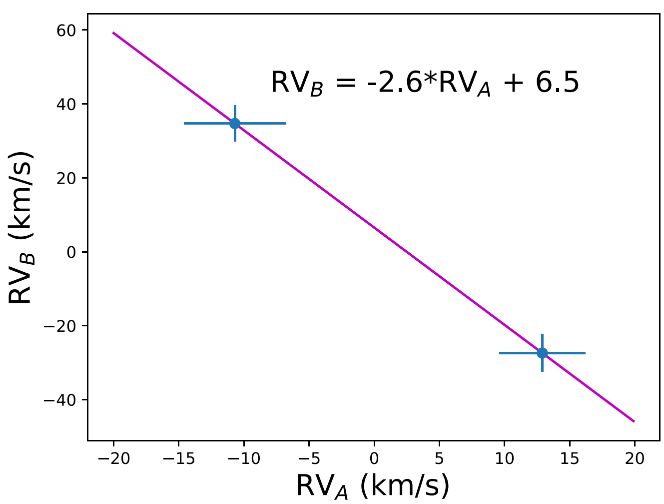

Figure 10. RV of component *B* as a function of the RV of component *A* for 2MASS J08355977−3042306.

A parallax measurement from Gaia (Gaia et al. 2016) indicates a distance of 62.7 ± 1.6 pc. Using this distance and the systemic RV, we calculate its UVW velocities as -9.9 ± 0.5, -3.6 ± 1.5, -15.8 ± 0.2 km s^{-1} and XYZ coordinates as -18.4 ± 1.0, -56.4 ± 3.1, 6.2 ± 0.3 pc.

Plotting these with the locations of YMG in both 3D velocity space and positional space (Figure 5), the system is not consistent with any known YMG. There are three likely possibilities for that; we explore each of those three options below.

1. If the system formed in a known YMG, it could have been ejected after formation due to three-body gravitational interactions (Sterzik & Durisen 1995). However, the initial interaction would produce a star with higher velocities ($\gtrsim$40 km s^{-1}) than 2MASS J08355977−3042306 has, so while we cannot rule out this option completely, it is the least likely scenario of the three (Perets & Subr 2012).
2. While most stars form in clusters (Evans 1999 and references therein), stars and binaries are capable of forming in isolated environments (Adams & Myers 2001). Based on the spatial distribution of young stellar objects, at least 10% of low-mass stars appear to form in isolation (Bressert et al. 2010). In this case, it would not have kinematics that matched with any other star's.
3. Surveys of low-mass stars are only complete to a distance of 25 pc (Shkolnik et al. 2012). Most stars in known YMGs are within 90 pc of the Sun (Malo et al. 2014). It is very possible that 2MASS J08355977−3042306 could be the first star in a currently unknown discovered YMG, much like TW Hydra once was.

Since it does not fit into any YMG, we questioned whether the system was truly young. RS CVn systems are close, active binaries, where at least one of the components is an evolved star (Hall 1976). They have lithium and large 10% velocity widths (Eker & Doherty 1987; Pallavicini et al. 1992; Bopp et al. 1993; Montes et al. 1995). However, while RS CVn systems have lithium, their EWs are less than 100 mÅ which is much less than that of 2MASS J08355977−3042306 (Neuhaeuser et al. 1997). Additionally, all currently identified RS CVn stars have spectral types earlier than that of 2MASS J08355977−3042306.

6.3. 2MASS J10260210−4105537

We acquired data in six epochs for this star—three from the du Pont and three from Magellan. All six epochs show resolved lithium absorption for both components (Figure 12). We measured a composite spectral type of M1.5 ± 0.5 for this system. The absorption features are wide and shallow, indicating that both components are relatively rapid rotators, which is common in young stars.

Five of the CCFs showed displaced velocity-resolved components (Figure 13). However, we were only able to calculate RVs from the CCF for three of the six epochs (Table 7), because we were unable to deblend the others due to a poor S/N and a lack of velocity separation between the components. After fitting a line to the data in the RV plot (Figure 14), we calculated a mass ratio of 0.59 ± 0.30, with the

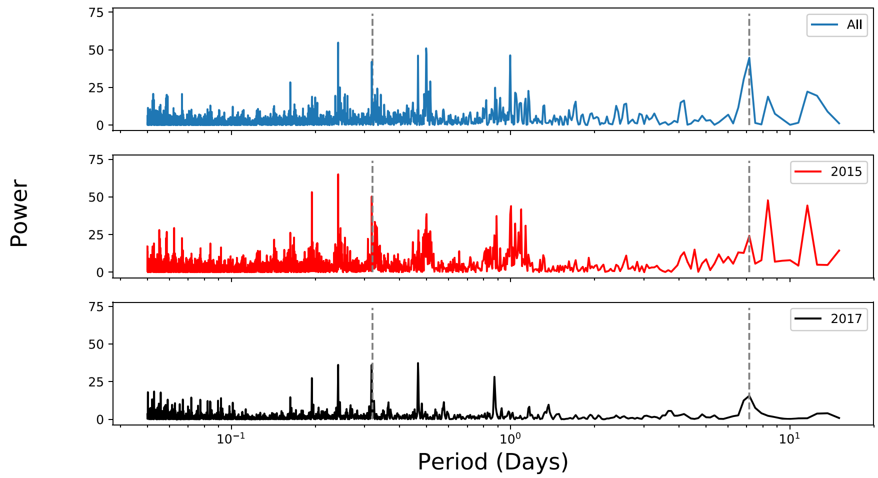

Figure 11. Periodograms for 2MASS J08355977−3042306 of the photometric data for all the data (top), just the 2015 data (middle), and just the 2017 data (bottom). Peaks at 0.32 and 7.15 days occur in all three.

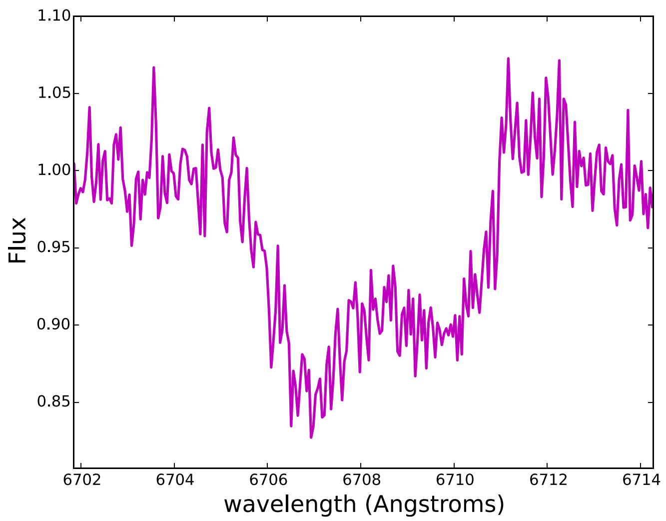

Figure 12. Lithium absorption at 6708 Å for 2MASS J10260210−4105537, with both components resolved. The presence of lithium puts an upper age limit on the system of 15 Myr.

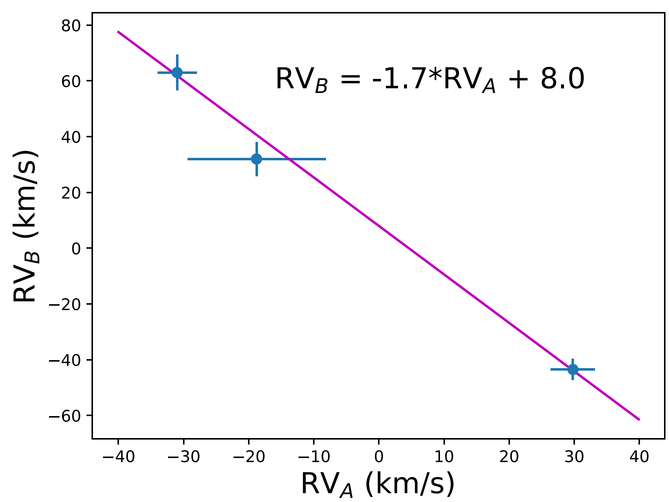

Figure 14. RV of component B as a function of the RV of component A for 2MASS J10260210−4105537. From this we calculated a mass ratio of 0.59 ± 0.30 and a systemic RV of 3.0 ± 3.5 km s^{-1}.

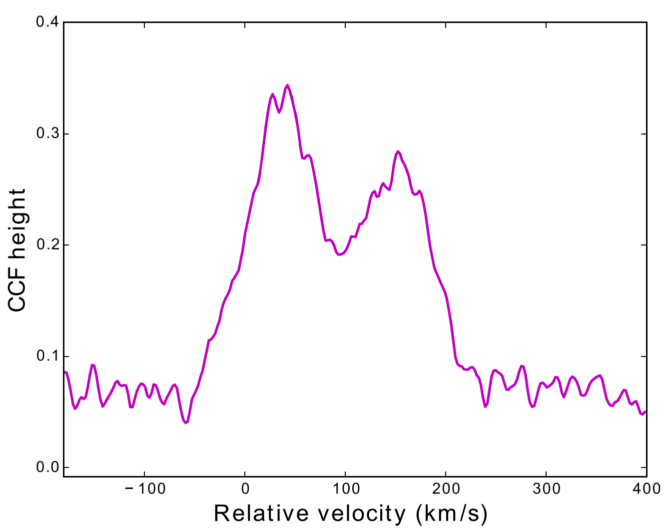

Figure 13. CCF for 2MASS J10260210−4105537 from 2009 December using GJ 908 as a template. The radial velocity of both components could be measured in this epoch.

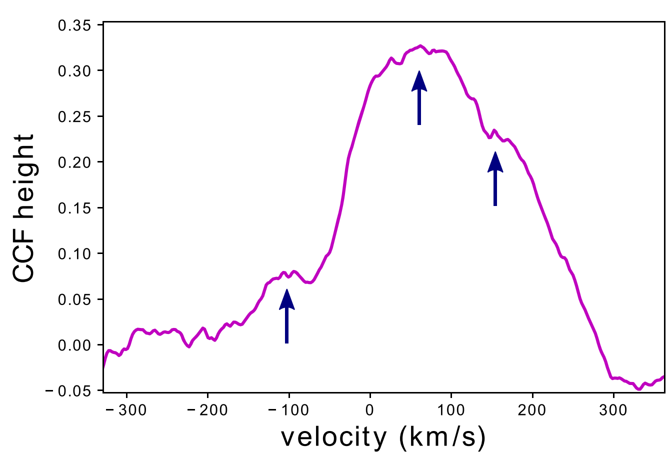

Figure 15. CCF from 2010 December showing indications of three stars.

primary at a mass of 0.50 $M_{\odot}$ and a spectral type of M0.9, which rounds to M1.0, and the secondary at a mass of 0.29 $M_{\odot}$ and a spectral type of M3.0. For stars with a mass of 0.5 $M_{\odot}$,

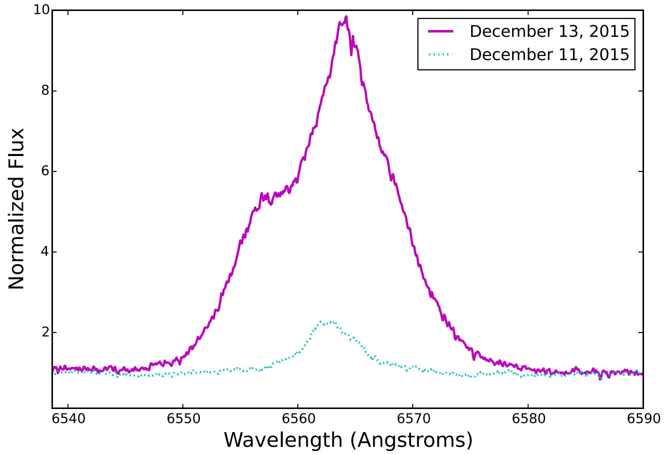

Figure 16. Hα emission for 2MASS J10260210−4105537 increases by an order of magnitude in two days.

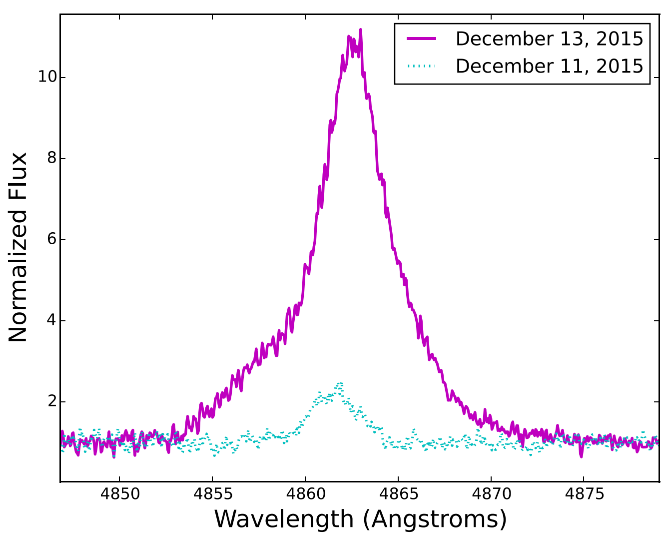

Figure 17. Hβ emission for 2MASS J10260210−4105537 increases by over an order of magnitude in two days due to chromospheric activity.

lithium is typically depleted by 15 Myr (Baraffe et al. 2015), putting an upper age limit on the system. The systemic RV is 3.0 ± 3.5 km s^{-1}. The large uncertainties are due to the broad CCF peaks. We calculate the upper limit of the period as 9.4 days and the upper limit of the semimajor axis as 0.08 au.

Using the distance of 84.9 ± 1.0 pc from Gaia DR2 along with our RV, we calculated UVW to be (-14.2 ± 0.4, -6.79 ± 3.4, -9.7 ± 0.9) km s^{-1} and XYZ to be (7.9 ± 0.1, -82.0 ± 1.0, 20.4 ± 0.2) pc. Based on both UVW and XYZ, the system does not appear to be a match for any YMG (Figure 5) or nearby star-forming regions (Mamajek 2015). While it fits well in Octans (≈20 Myr) in UVW space, it does not match in XYZ space. This young binary is another relatively distant, isolated, young system.

However, there are indications in the spectra and CCF, particularly the one from 2010 December (Figure 15), that this system may in reality be a triple system. While we believe this to be fairly unlikely as evidence is not seen in several other epochs, if true, the calculated RV and UVW velocities would

Table 7
RVs for J10260210−4105537

UT Date	RV of *A* (km s^{-1})	RV of *B* (km s^{-1})
2009 Jun 14	−31.0 ± 3.0	63.0 ± 6.4
2009 Dec 31	29.8 ± 3.4	−43.5 ± 3.8
2015 Dec 11	−18.8 ± 10.6	32.0 ± 6.1

not be accurate, as they are calculated based on the gravitational interactions between two bodies. In that case, the system may fit into a YMG.

6.3.1. Spectral Features and Flare Activity

Hα is in emission in all of the spectra for 2MASS J10260210 −4105537. The EW of Hα ranged from −8 to −10 Å in the first five epochs. These values make it unlikely that the star is still accreting (White & Basri 2003).

However, in the final epoch from 2015 December 13, which was taken only two days after the previous one, its EW was −92 Å (Figure 16). Comparable increases occurred in all of the hydrogen Balmer series features (Figure 17) and helium features at 4471, 4921, 5018, 5876, and 6678 Å. Additionally, other features that were in absorption on 2015 December 11 were in emission on 2015 December 13, such as Fe II at 5169 Å, Fe I at 5328 Å, the Na I doublet at 5890 and 5896 Å, O I at 7773 Å, and the Ca II triplet (Figure 18) at 8498, 8542, and 8662 Å.

The cause of activity cannot be determined from the data we have now. Possible causes include regular activity from one or both stars typically seen in young, low-mass stars (Noyes et al. 1984), although generally not at this level. It could also be due to the interactions between the binaries (Brandner et al. 1996). And while it does not appear to be actively accreting and there is no IR excess, there could still be brief accretion events. Further observations are needed to determine the frequency and magnitude of these events to have a better understanding of the cause.

7. Conclusions

In this paper, we present three new young, low-mass SBs discovered with high-resolution optical spectra. Using the component RVs we measured for each epoch, we calculated mass ratios and the systemic RVs for all three SBs. Using the systemic RVs with their coordinates and proper motions, we calculated full 3D velocities to search for potential membership of known YMGs. We also determined the masses and spectral types for the individual components. For 2MASS J02543316 −5108313 our RV measurements confirmed the Tuc-Hor membership from Kraus et al. (2014). All characteristics, including the lack of lithium, are consistent with Tuc-Hor's age of 40 Myr. 2MASS J08355977−3042306 is an SB2 with lithium in both components. This puts an upper age limit of 15 Myr on the system. Despite this, it does not fit kinematically with any known YMG. 2MASS J10260210−4105537 was previously known to be young based on its lithium absorption and was a potential TWA member. However, it too does not fit with any known moving group based on its kinematics. It is possible that these two "homeless systems" are the first stars to be discovered in new YMGs that are <15 Myr old and only ≈60–100 pc away. Discovering new, nearby YMGs associated

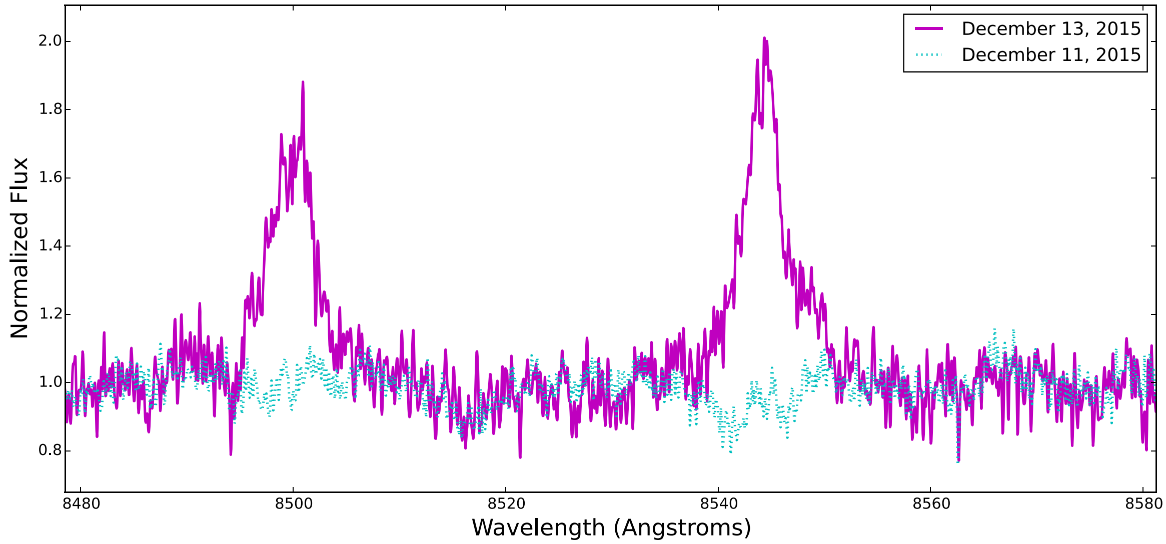

Figure 18. Two lines of the Ca II triplet for 2MASS J10260210−4105537 were in absorption on 2015 December 11, but emission on 2015 December 13.

with these two young SBs, as has been done for other stars post-Gaia (e.g., Faherty et al. 2018), would be valuable for developing a more complete understanding of the evolution of low-mass stars.

This work was supported by the NASA/Habitable Worlds grant NNX16AB62G (PI E. Shkolnik). B.P.B. acknowledges support from the National Science Foundation grant AST-1909209. L.F. would like to thank Lisa Prato for many helpful discussions and Joleen Carlberg for patiently guiding me though the spectroscopic data reduction process for the first time. This research has made use of the VizieR catalog access tool, CDS, Strasbourg, France (Wenger et al. 2000). The original description of the VizieR service was published in A&AS 143, 23. This research has made use of the SIMBAD database,operated at CDS, Strasbourg, France (Wenger et al. 2000). This research has made use of the NASA/IPAC Infrared Science Archive, which is operated by the Jet Propulsion Laboratory, California Institute of Technology, under contract with the National Aeronautics and Space Administration. This work has made use of data from the European Space Agency (ESA) mission Gaia (https://www.cosmos.esa.int/gaia), processed by the Gaia Data Processing and Analysis Consortium (DPAC, https://www.cosmos.esa.int/web/gaia/dpac/consortium). Funding for the DPAC has been provided by national institutions, in particular the institutions participating in the Gaia Multilateral Agreement.

ORCID iDs

Laura Flagg https://orcid.org/0000-0001-6362-0571
Evgenya L. Shkolnik https://orcid.org/0000-0002-7260-5821
Alycia Weinberger https://orcid.org/0000-0001-6654-7859
Brendan P. Bowler https://orcid.org/0000-0003-2649-2288
Adam L. Kraus https://orcid.org/0000-0001-9811-568X
Michael C. Liu https://orcid.org/0000-0003-2232-7664

References

Adams, F. C., & Myers, P. C. 2001, ApJ, 553, 744
Baraffe, I., Homeier, D., Allard, F., & Chabrier, G. 2015, A&A, 577, A42
Barrado y Navascués, D., & Martín, E. L. 2003, AJ, 126, 2997
Bergfors, C., Brandner, W., Janson, M., et al. 2010, A&A, 520, A54
Bernstein, R., Shectman, S. A., Gunnels, S. M., Mochnacki, S., & Athey, A. E. 2003, Proc. SPIE, 4841, 1694
Bianchi, L., Herald, J., Efremova, B., et al. 2011, Ap&SS, 335, 161
Bochanski, J. J., Hawley, S. L., Covey, K. R., et al. 2010, AJ, 139, 2679
Bonsack, W. K. 1959, ApJ, 130, 843
Bonsack, W. K., & Greenstein, J. L. 1960, ApJ, 131, 83
Bopp, B. W., Fekel, F. C., Aufdenberg, J. P., Dempsey, R., & Dadonas, V. 1993, AJ, 106, 2502
Bowler, B. P., Hinkley, S., Ziegler, C., et al. 2019, ApJ, 877, 60
Brandner, W., Alcala, J. M., Kunkel, M., Moneti, A., & Zinnecker, H. 1996, A&A, 307, 121
Bressert, E., Bastian, N., Gutermuth, R., et al. 2010, MNRAS, 409, L54
Brown, A. G. A., Vallenari, A., Prusti, T., & de Bruijne, J. H. J. 2018, A&A, 616, A1
Chabrier, G., & Baraffe, I. 1997, A&A, 327, 1039
Crockett, C. J., Mahmud, N. I., Prato, L., et al. 2012, ApJ, 761, 164
Dib, S. 2014, MNRAS, 444, 1957
Dressing, C. D., & Charbonneau, D. 2013, ApJ, 767, 95
Eker, Z., & Doherty, L. R. 1987, MNRAS, 228, 869
Evans, N. J., II 1999, ARA&A, 37, 311
Faherty, J. K., Bochanski, J. J., Gagné, J., et al. 2018, ApJ, 863, 91
Feiden, G. A., & Chaboyer, B. 2012, ApJ, 757, 42
Fitzpatrick, M. J. 1993, in ASP Conf. Ser. 472, adass II, 472, ed. R. J. Hanisch, R. J. V. Brissenden, & J. Barnes (San Francisco, CA: ASP), 472
Fleming, D. P., Barnes, R., Davenport, J. R. A., & Luger, R. 2019, ApJ, 881, 88
Gaia Collaboration, Prusti, T., de Bruijne, J. H. J., et al. 2016, A&A, 595, A1
Gagné, J., Faherty, J. K., Mamajek, E. E., et al. 2017, ApJS, 228, 18
Gagné, J., Lafrenière, D., Doyon, R., Malo, L., & Artigau, É. 2015, ApJ, 798, 73
Hall, D. S. 1976, ASSL, 60, 287
Hoadley, K., France, K., Alexander, R. D., McJunkin, M., & Schneider, P. C. 2015, ApJ, 812, 41
Horne, J. H., & Baliunas, S. L. 1986, ApJ, 302, 757
Janson, M., Hormuth, F., Bergfors, C., et al. 2012, ApJ, 754, 44
Johnson, D. R. H., & Soderblom, D. R. 1987, AJ, 93, 864
Kass, R. E., & Raftery, A. E. 1995, J. Am. Stat. Assoc., 90, 773
Kelson, D. D. 2003, PASP, 115, 688
Kiraga, M. 2012, AcA, 62, 67
Kirkpatrick, J. D., Henry, T. J., & McCarthy, D. W., Jr. 1991, ApJS, 77, 417
Kraus, A. L., Shkolnik, E. L., Allers, K. N., & Liu, M. C. 2014, AJ, 147, 146
Krzesinski, J., Baran, A. S., Winiarski, M., et al. 2012, AcA, 62, 201
Linsky, J. L. 1980, ARA&A, 18, 439
Liu, M. C., Dupuy, T. J., & Allers, K. N. 2016, ApJ, 833, 96
Luri, X., Brown, A. G. A., Sarro, L., et al. 2018, A&A, 616, A9
Malo, L., Artigau, É., Doyon, R., et al. 2014, ApJ, 788, 81
Mamajek, E. E. 2015, UV Galactic Velocity Vectors for Nearby Young Stellar Groups, http://www.pas.rochester.edu/~emamajek/images/uvw_young_groups.jpg
Martin, D. C., Fanson, J., Schiminovich, D., et al. 2005, ApJL, 619, L1

Montes, D., Fernandez-Figueroa, M. J., de Castro, E., & Cornide, M. 1995, A&AS, 109, 135
Montes, D., López-Santiago, J., Gálvez, M. C., et al. 2001, MNRAS, 328, 45
Montes, D., Martin, E. L., Fernandez-Figueroa, M. J., Cornide, M., & de Castro, E. 1997, A&AS, 123, 473
Murray, C. A. 1989, A&A, 218, 325
Naud, M.-E., Artigau, É., Doyon, R., et al. 2017, AJ, 154, 129
Neuhaeuser, R., Torres, G., Sterzik, M. F., & Randich, S. 1997, A&A, 325, 647
Nidever, D. L., Marcy, G. W., Butler, R. P., Fischer, D. A., & Vogt, S. S. 2002, ApJS, 141, 503
Noyes, R. W., Hartmann, L. W., Baliunas, S. L., Duncan, D. K., & Vaughan, A. H. 1984, ApJ, 279, 763
Pallavicini, R., Randich, S., & Giampapa, M. S. 1992, A&A, 253, 185
Pecaut, M. J., & Mamajek, E. E. 2013, ApJS, 208, 9
Perets, H. B., & Subr, L. 2012, ApJ, 751, 133
Pojmanski, G. 2002, AcA, 52, 397
Rebull, L. M., Stauffer, J. R., Cody, A. M., et al. 2018, AJ, 155, 196
Reid, I. N., & Gizis, J. E. 1997, AJ, 113, 2246
Reid, I. N., Hawley, S. L., & Gizis, J. E. 1995, AJ, 110, 1838
Riaz, B., Gizis, J. E., & Harvin, J. 2006, AJ, 132, 866
Rodriguez, D. R., Bessell, M. S., Zuckerman, B., & Kastner, J. H. 2011, ApJ, 727, 62
Rodriguez, D. R., Zuckerman, B., Kastner, J. H., et al. 2013, ApJ, 774, 101
Schlieder, J. E., Lépine, S., & Simon, M. 2010, AJ, 140, 119
Schlieder, J. E., Lépine, S., & Simon, M. 2012, AJ, 144, 109
Schneider, A. C., Shkolnik, E. L., Allers, K. N., et al. 2019, AJ, 157, 234
Shan, Y., Yee, J. C., Bowler, B. P., et al. 2017, ApJ, 846, 93
Shkolnik, E. L., Allers, K. N., Kraus, A. L., Liu, M. C., & Flagg, L. 2017, AJ, 154, 69
Shkolnik, E. L., Anglada-Escudé, G., Liu, M. C., et al. 2012, ApJ, 758, 56
Shkolnik, E. L., Liu, M. C., Reid, I. N., Dupuy, T., & Weinberger, A. J. 2011, ApJ, 727, 6
Skrutskie, M. F., Cutri, R. M., Stiening, R., et al. 2006, AJ, 131, 1163
Skumanich, A. 1972, ApJ, 171, 565
Soderblom, D. R., King, J. R., & Henry, T. J. 1998, AJ, 116, 396
Somers, G., & Pinsonneault, M. H. 2015, ApJ, 807, 174
Spangler, C., Sargent, A. I., Silverstone, M. D., Becklin, E. E., & Zuckerman, B. 2001, ApJ, 555, 932
Spiegel, D. S., & Burrows, A. 2012, ApJ, 745, 174
Sterzik, M. F., & Durisen, R. H. 1995, A&A, 304, L9
Tody, D. 1986, SPIE, 627, 733
Tokovinin, A., Fischer, D. A., Bonati, M., et al. 2013, PASP, 125, 1336
Tonry, J., & Davis, M. 1979, AJ, 84, 1511
Torres, C. A., Da Silva, L., Quast, G. R., De La Reza, R., & Jilinski, E. 2000, AJ, 120, 1410
Torres, C. A. O., Quast, G. R., da Silva, L., et al. 2006, A&A, 460, 695
Virtanen, P., Gommers, R., Oliphant, T. E., et al. 2019, arXiv:1907.10121
Voges, W., Aschenbach, B., Boller, T., et al. 1999, A&A, 349, 389
Walter, F. M., Brown, A., Mathieu, R. D., Myers, P. C., & Vrba, F. J. 1988, AJ, 96, 297
Wenger, M., Ochsenbein, F., Egret, D., et al. 2000, A&AS, 143, 9
White, R. J., & Basri, G. 2003, ApJ, 582, 1109
Williams, J. P., & Cieza, L. A. 2011, ARA&A, 49, 67
Wilson, O. C. 1941, ApJ, 93, 29
Wright, E. L., Eisenhardt, P. R. M., Mainzer, A. K., et al. 2010, AJ, 140, 1868
Zacharias, N., Finch, C. T., Girard, T. M., et al. 2013, AJ, 145, 44
Zuckerman, B., & Song, I. 2004, ARA&A, 42, 685